





RESEARCH ARTICLE | DECEMBER 11 2023

Quasi-BIC high-index resonators for liquid characterization and analysis

Ildar Yusupov ; Dmitry Dobrykh ; Polina Terekhina ; Dmitry Filonov ; Pavel Ginzburg ; Mikhail V. Rybin ; Alexey Slobzhanyuk 

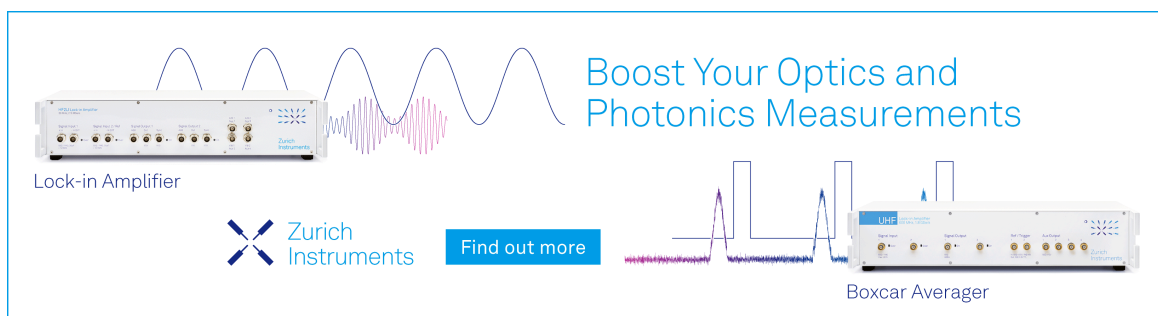
 Check for updates

Appl. Phys. Lett. 123, 244102 (2023)

<https://doi.org/10.1063/5.0170786>




CrossMark



Boost Your Optics and Photonics Measurements

Lock-in Amplifier

 Zurich Instruments

[Find out more](#)

Boxcar Averager

Quasi-BIC high-index resonators for liquid characterization and analysis

Cite as: Appl. Phys. Lett. **123**, 244102 (2023); doi: [10.1063/5.0170786](https://doi.org/10.1063/5.0170786)

Submitted: 4 August 2023 · Accepted: 26 November 2023 ·

Published Online: 11 December 2023



View Online



Export Citation



CrossMark

Ildar Yusupov,^{1,a)}  Dmitry Dobrykh,^{2,3}  Polina Terekhina,¹  Dmitry Filonov,⁴  Pavel Ginzburg,² 
Mikhail V. Rybin,^{1,5}  and Alexey Slobozhanyuk¹ 

AFFILIATIONS

¹School of Physics and Engineering, ITMO University, Saint Petersburg, Russia

²School of Electrical Engineering, Tel Aviv University, Tel-Aviv, Israel

³Qingdao Innovation and Development Center, Harbin Engineering University, Qingdao, Shandong, China

⁴Center for Photonics and 2D Materials, Moscow Institute of Physics and Technology, Dolgoprudny, Russia

⁵Ioffe Institute, Saint Petersburg, Russia

^{a)} Author to whom correspondence should be addressed: ildar.yusupov@metalab.ifmo.ru

ABSTRACT

Capabilities to monitor the purity and mixture composition of liquids with the aid of low-cost portable devices can grant essential advantages in maintaining personal health safety. The overwhelming majority of consumer wireless devices operate at relatively small operational bandwidth, thus not allowing for retrieving material composition via dispersion characteristics. To mitigate the bandwidth limitations, resonant methods, granting precision in a small frequency window, might be of use. Here, we demonstrate a liquid sensor able to provide 90.5 kHz/RIU sensitivities owing to a resonator, supporting high-quality factor quasi-bound states in the continuum. The sensor's architecture encompasses a high-permittivity ceramic resonator and a capillary wrapped around it. The volumetric design increases the overlap between the electromagnetic mode and the liquid under test while maintaining resonant conditions within a relatively narrow frequency band. To demonstrate the capabilities of the proposed method, the UHF RFID band was considered, and temperature dependence of the distilled water permittivity was retrieved. Interfacing standalone low-cost electromagnetic sensors with widely available consumer-level wireless devices offers promising opportunities that contribute to the paradigm shift toward IoT.

Published under an exclusive license by AIP Publishing. <https://doi.org/10.1063/5.0170786>

Modern decision-making systems rely on multiple sensors, capable of performing real-time monitoring of environmentally relevant parameters.¹ Typically, sensors are designed to measure temperatures, humidities, compositions, and other parameters of gases and liquids. This information is then used for decision-making.^{2,3} In many industrial applications, sensors are employed to characterize the dielectric properties of solid and liquid chemicals.⁴ Microfluidic sensors play a crucial role in biomedical research by enabling the extraction of liquid parameters without a need for biomarkers.⁵ Biosensors are particularly useful in analyzing fluid composition, e.g., blood, which assists in performing a disease diagnosis and increases treatment capabilities.⁶ An efficient sensor network can significantly reduce the time and cost of research and industrial production. Herein, we will concentrate on low-cost wireless liquid sensors.

A liquid under test (LUT) interacts with a sensor, which extracts information on the material composition by changing a probe response. Among a variety of existent methods, spectroscopy is

considered among the most accurate ones. On pathways to reduce device costs and keep sensors on a consumable level, many architectures have been developed. There are two main spectroscopy-based approaches for sensing, i.e., (i) a resonant and (ii) non-resonant. The first one depends on a core resonant structure, which supports high-quality factor (high-Q) resonances at a discrete set of frequencies. Non-resonant architectures benefit from low-Q broadband probes, which are less sensitive compared to high-Q counterparts. Typical examples of these methods are sensors based on split-ring resonators (SRR) and waveguides.^{7–11} Among the family of resonant probes, dielectric resonators¹² have many advantages, as has been demonstrated in several reports.^{13,14} As a rule of thumb, the main requirement from a high-quality probe is to demonstrate a significant response to small changes in a measured parameter. In this endeavor, developing high-Q resonators with environmentally sensitive resonances is the way to go. Typical values of achievable Q-factors for planar structures can range from tens to hundreds, e.g., 525 in Ref. 15. For

structures based on surface impedance, waveguides¹⁶ can grant a Q-factor as high as a few hundred. Dielectric resonator-based sensors demonstrate similar performances.¹³ Table S1 summarizes several passive architectures, emphasizing achievable Q-factors. It is worth noting that introducing active schemes can significantly elevate performances at the expense of cost and complexity. For example, a Q-factor as high as 13 000 was reported for active SRR-based geometries.¹⁷ Another appealing approach is to increase a device's electrical size. A whispering gallery mode-based optical resonators demonstrate a superior sensitivity owing to their exceptionally high-Q.¹⁸ However, those optical architectures cannot be scaled down to MHz–GHz spectral range since a device footprint, encompassing multiple wavelengths over the circumference, will have an unreasonably large footprint. Consequently, the challenge is to find architectures capable of (i) compatibility with existent wireless devices, operating at MHz–GHz frequency bands, (ii) having a small (portable) footprint, and (iii) demonstrating moderately high-Q resonances.

Bound states in the continuum (BIC) address the previously mentioned demands. BIC phenomenon, being initially proposed as a mathematical concept in quantum mechanics almost a century ago, was generalized to many other fields, including classical electrodynamics.^{19–21} The essence of this effect is an interference prohibiting coupling of a resonant bound mode and the radiation continuum.^{22,23} Destructive interference between a pair of resonant leaky modes leads to the emergence of high-Q hybridized resonance with signatures resembling quasi-BIC or supercavity modes.²⁴ Since quasi-BIC in dielectric resonators possess a Q-factor on the order of several thousands,²⁵ it is appealing to exploit them in sensing. Several proposals already utilized quasi-BIC modes for lasing,²⁶ sensing of biological objects,²⁷ refractometry,²⁸ and temperature measurements.²⁹

In this Letter, we demonstrate a portable microwave sensor, capable retrieving dielectric parameters of liquids at a high accuracy. The main element of the device is a dielectric resonator, which supports a high-Q supercavity mode. To elucidate the impact of the quasi-BIC concept, we compare the supercavity mode with the magnetic dipole, which is typically used in classical resonators. The device performances are assessed vs a high-grade active commercial apparatus. Distilled water at different temperatures is used as a LUT.

While a variety of different electromagnetic structures supporting quasi-BIC were investigated,²⁹ high-permittivity cylinders might be considered as a compromise for an optimization task. Cylinder is a relatively simple geometric structure, which have enough independent degrees of freedom, sufficient to control its properties and preserve compact dimensions, given refractive index is high. Ceramic materials with unique properties, created through the mixing of powders and subsequent sintering under pressure, allow to treat permittivity as an independent degree of freedom. Moreover, the high real part of permittivity, reaching into the hundreds or even thousands, does not entail the drawback of elevated material losses; these losses are kept reasonably low, enabling the resonator to support high-Q modes. Based on similar considerations, dielectric resonant antennas (DRA) were developed to address several challenges of metallic antennas, e.g., to sustain high power and support a sufficient bandwidth given a small footprint.³⁰ However, in an overwhelming majority of cases, permittivity above 10 is rarely considered owing to bandwidth limitations, losses, and several technological aspects.³¹ To support several modes within a small footprint structure, a higher permittivity is typically required.

Supercavity modes in a high-permittivity dielectric resonator emerge when two modes (typically, Mie and Fabry–Pérot resonances) being nearly orthogonal within the interior strongly interact in the free space. This effect leads to the so-called avoid-crossing pattern. A destructive interference appears between the mode leaking tails outside the resonator. Given the set of properly chosen parameters, a quasi-BIC state emerges.^{24,32} To find quasi-BIC states, we performed a series of full-wave numerical simulations using the frequency domain solver in the CST Microwave Studio. The resonator was excited with a plane wave, and the total scattering cross section and near-field distributions were analyzed to identify TE_{020} , TE_{012} , and the resulting quasi-BIC modes. TE_{mnk} mode classification is the standard notation. Transverse electric (TE) modes have a vanishing longitudinal (E_z is along the cylinder axis) component, where m is the azimuthal number ($m = 0$ in our case, as the mode is symmetric), n is the radial number, where $n - 1$ is the number of nodes along the radial coordinate, and k is the longitudinal number of nodes along the z axis.³² Considering this mode classification, TE_{020} is attributed to Mie resonances, while TE_{012} is a Fabry–Pérot standing wave—both are leaky and hence are coupled with their tails in the free space.

Considering the fabrication aspects and the layout of the proposed sensor device (Fig. 1), the aspect ratio between the cylinder radius (r) and height (h) was chosen as ~ 0.7 , which is close to previously reported geometries, supporting quasi-BIC modes.²⁵ After the parametric study, the optimal parameters of the resonator were found to be $r = 30.8$, $h = 44.6$ mm, and dielectric permittivity $\epsilon = 100$ with a loss tangent of 10^{-4} (corresponding to experimental data, which will follow). These parameters enable obtaining the quasi-BIC mode inside the UHF RFID frequency range 902–928 MHz (US band). Since the operational bandwidth of the sensor is rather narrow, material dispersion can be neglected. Worth noting that the figure of merit here is comparing the sensor's footprint with the free space wavelength. Though, for practical applications, the device shall be equipped with special holders encompassing the excitation source and other peripherals, making the overall size bigger.

The optimized parameters of the cylindrical resonator, supporting the quasi-BIC mode, are used for the sensor design. Since the quasi-BIC mode has the axial symmetry, a capillary is wrapped around the resonator to maximize the interaction with the electric field. The choice of a 3 mm radius for the tube is a compromise between the electromagnetic sensitivity and the capability to pump fluids easily through the cross section. Consequently, the volume of liquid that can be contained in one coil of the tube is 217 μL .

The LUT volume, interacting with the resonator, directly affects the mode profile and, as the result, the sensitivity. To determine the optimal number of wrapped tubes (or number of coils) for maximizing the sensitivity, a numerical analysis has been conducted. For the assessment, the resonator was illuminated with a plane wave, and the forward scattering was used to probe the modal response (the electric field maps are presented in Fig. S1 in the supplementary material). Experimentally retrieved complex-valued parameters of distilled water (the LUT, Fig. S2 in the supplementary material) as the function of temperature were used. By observing the change in permittivity and loss tangent corresponding to temperature, we revealed the dynamics of the resonant response, examining 1, 3, 5, 7, and 9 coils wrapped around the resonator. We observed that with fewer than five coils, the frequency and amplitude shift is insufficient due to weak coupling

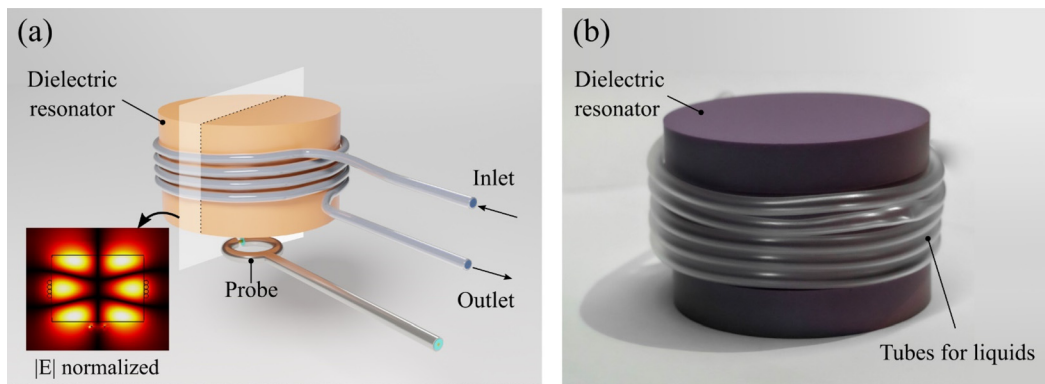


FIG. 1. (a) The sensor layout, consisting of the dielectric cylinder and the capillary wrapped around. The cylinder supports a quasi-BIC state (electric field amplitude distribution displayed in the inset), which is probed by the small loop antenna placed underneath the device. Liquid under test is pumped through the capillary. (b) The photograph of the sensor device.

between the resonator and the analyte. On the other hand, with 7 and 9 coils, the sensor sensitivity worsened due to degradation of the quasi-BIC mode. Table I shows the results of numerical simulation estimating the sensitivity of the sensor, responding to a change of LUT permittivity by 10 units (from 73 to 63, for the sake of the assessment).

While quasi-BIC modes can be excited via both near- and far-field sources,²⁹ near-field excitation with a loop has an advantage in terms of the signal-to-noise ratio. In this case, the free-space propagation and associated additive noises are eliminated. Hereinafter, a small metallic loop antenna with a radius of $r_{pr} = 4$ mm and a discrete 50 Ω port is used as a source. The loop is placed 6 mm apart from the resonator. This distance is the result of an optimization (refer to Fig. S3 in the supplementary material). Figure 2(a) shows the impact of the LUT dielectric permittivity change on the reflection coefficient of the probe ($|S_{11}|$). Color lines are the numerically obtained spectra for several different temperatures of the liquid. The $|S_{11}|$ spectra are investigated for the dipole and quasi-BIC modes. While the frequency shift for both of the modes is almost the same, the quasi-BIC demonstrates a significant change in Q-factor.

To demonstrate the concept experimentally, we fabricated a cylindrical resonator made of low-loss ceramics. $\text{BaLa}_2\text{Ti}_4\text{O}_{12}$ material was chosen owing to its refractive index temperature stability,³³ thus the LUT does not change its electromagnetic properties. The fabricated sample has $\epsilon = 102.34$, and a loss tangent of 4×10^{-4} . It is worth noting that a ceramic material with a higher permittivity can potentially elevate the Q-factor and thus the sensitivity. However, a potential temperature dispersion might overcomplicate the data analysis, favoring the use of temperature-stable materials. The quasi-BIC was excited by a small loop probe antenna placed under the cylinder at a distance of 6 mm, as illustrated schematically in Fig. 1(a) and photographed in Fig. 3(c). The resonator was placed on a Styrofoam with a dielectric permittivity of approximately 1.1 and negligible losses. A medical drip

tube with a diameter of 3 mm was wrapped around the resonator [see Figs. 1(b) and 3(c)]. One end of the tube was connected to a jar with the LUT, and the other end was connected to a syringe with which the fluid was pumped into the channel. The temperature was measured using an infrared thermometer directed at the drip tube. The measurement on the initially heated fluid continued until the temperature reached room conditions. The reflection coefficient spectra measured by a Ceyear 3656B vector network analyzer (VNA) are presented in Fig. 2(b). Two modes of the dielectric resonator, namely, the magnetic dipole (at 447 MHz) and quasi-BIC (around 914 MHz), were monitored. Differences between numerical and experimental results are due to the loop antenna backend, which is difficult to reproduce in simulations. Other contributing factors are the deviations in dielectric parameters of both the LUT and the ceramics.

Using the retrieved parameters of water (refer to Fig. S2 in the supplementary material), we attribute changes in dielectric permittivity and loss tangent by 9.5 (from 63.3 to 72.8) in response to the heating from 64 to 36 °C. Those dielectric changes shift the resonant frequency of dipole mode from 449.7 to 449.022 MHz and quasi-BIC mode from 914.59 to 913.73 MHz [Fig. 3(a)]. An estimation of the Q-factor change was also performed for a precise evaluation of the sensor performance since the temperature change also leads to an increase in the loss tangent. After fitting the data to a Lorentzian shape, the Q-factor was calculated [Fig. 3(b)]. The quasi-BIC mode is characterized by a more significant change of the Q-factor, compared to the dipole mode. The Q-factor of the tracked quasi-BIC shows the shift from 900 to 696, when the sensor interacts with the heated water.

Using the measured data, we calculated the sensitivity of the proposed sensor as the ratio of changes in water dielectric permittivity to the resonant frequency. In the next step, we conducted a parametric study by varying the number of wrapped coils. We experimentally measured the combinations of 1, 3, and 5 coils, and for each, we

TABLE I. Numerically calculated resonance frequency shift for different numbers of coils around the resonator.

Number of coils	One coil	Three coils	Five coils	Seven coils	Nine coils
Frequency shift with the change in $\Delta\epsilon_{LUT} = 10$	0.57 MHz	1.33 MHz	1.43 MHz	1.37 MHz	1.32 MHz

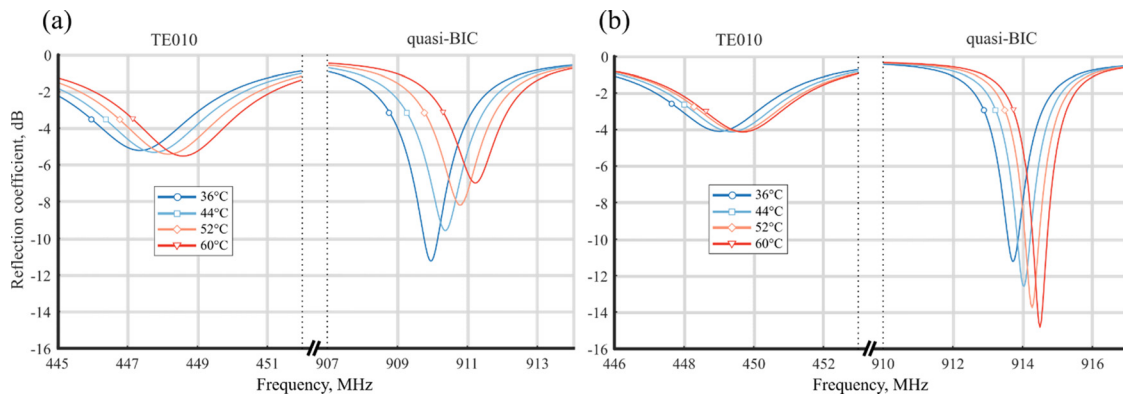


FIG. 2. Numerically (a) and experimentally (b) measured $|S_{11}|$ spectra for different temperatures of the water.

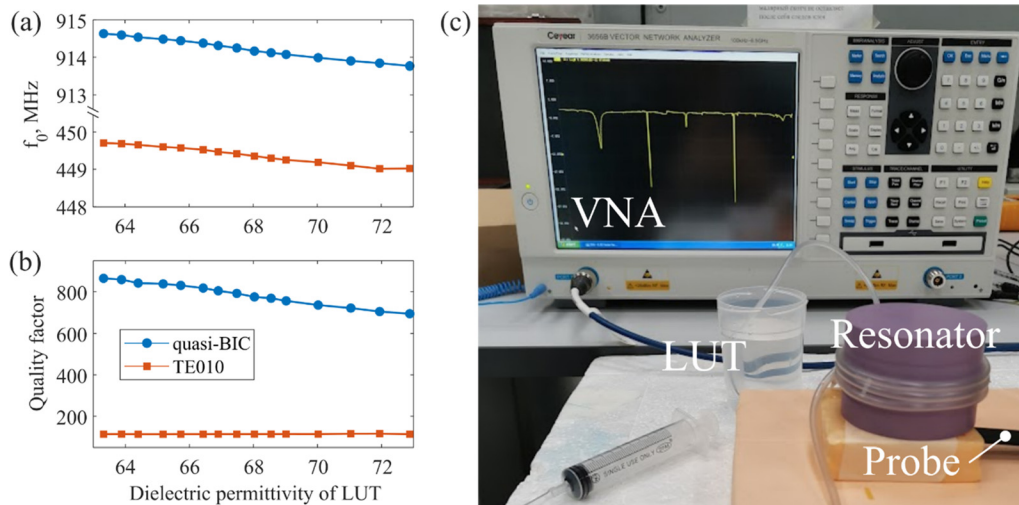


FIG. 3. Experimentally measured resonant frequency (a) and quality factor (b) vs dielectric permittivity of liquid under test. (c) Measurement setup.

calculated the sensitivity. Sensitivity was determined by calculating the difference between the resonant frequencies of the quasi-BIC or the Q-factor in relation to the contrast in dielectric permittivities, as described by the following equations:

$$S_f = \frac{\Delta f_0}{\Delta \epsilon},$$

$$S_Q = \frac{\Delta Q}{\Delta \epsilon}.$$

Calculated sensitivities are presented in Table II. The best performance for both sensitivities is higher when a five-coil setup is used.

In this work, the portable microwave sensor for estimating liquid dielectric parameters with high precision has been proposed. The sensor has a simple design consisting of a single ceramic resonator whose parameters are optimized to support supercavity mode with high-Q factor and high-dielectric permittivity to preserve compact dimensions. The liquid pumped through the tubes, wrapped around the resonator, has been monitored by observing the shift of the supercavity mode

TABLE II. Calculated sensitivities for different numbers of coils wrapped around the resonator.

	One coil		Three coils		Five coils	
	S_f (kHz/RIU)	S_Q ($\Delta Q/\Delta \epsilon$)	S_f (kHz/RIU)	S_Q ($\Delta Q/\Delta \epsilon$)	S_f (kHz/RIU)	S_Q ($\Delta Q/\Delta \epsilon$)
TE ₀₁₀	10.4	1.68	11.5	0.36	71.7	0.017
Quasi-BIC	14.6	9.2	18.8	11.13	90.5	20.6

resonant frequency. The five-coil setup shows the sensitivity as high as 90.5 kHz/RIU. The performance can be further improved by exploring materials with higher dielectric permittivity, which will also allow a significant miniaturization of the sensor.

See the supplementary material for the numerical analysis of the optimal position for quasi-BIC excitation, calibration data, and the comparison of passive sensors.

This work was supported by the Russian Science Foundation under Project No. 19-79-10232. The development of ceramic materials used in the experiment and optimization of the coil position was supported by state Assignment No. FSER-2022-0010 within the framework of the national project “Science and Universities.”

AUTHOR DECLARATIONS

Conflict of Interest

The authors have no conflicts to disclose.

Author Contributions

Ildar Yusupov: Investigation (equal); Visualization (equal); Writing – original draft (equal). **Dmitry Dobrykh:** Investigation (equal); Validation (equal); Visualization (equal); Writing – original draft (equal). **Polina Terekhina:** Investigation (equal); Visualization (equal). **Dmitry Filonov:** Methodology (equal). **Pavel Ginzburg:** Supervision (equal); Writing – review & editing (equal). **Mikhail Rybin:** Supervision (equal); Writing – review & editing (equal). **Alexey P. Slobozhanyuk:** Project administration (equal); Supervision (equal); Writing – review & editing (equal).

DATA AVAILABILITY

The data that support the findings of this study are available from the corresponding author upon reasonable request.

REFERENCES

- 1 A. Al-Fuqaha, M. Guizani, M. Mohammadi, M. Aledhari, and M. Ayyash, *IEEE Commun. Surv. Tutorials* **17**, 2347 (2015).
- 2 C. Shi, A. Rani, B. Thomson, R. Debnath, A. Motayed, D. E. Ioannou, and Q. Li, *Appl. Phys. Lett.* **115**, 121602 (2019).
- 3 H. You, D. Wu, J. Wang, J. He, X. Kuang, C. Li, F. Guo, D. Zhang, Q. Qi, and X. Tang, *Appl. Phys. Lett.* **122**(16), 162103 (2023).
- 4 R. A. Alahnomi, Z. Zakaria, Z. M. Yussof, A. A. Althuwayb, A. Alhegazi, H. Alsariera, and N. A. Rahman, *Sens. Rev.* **21**, 2267 (2021).
- 5 N. Navaratna, Y. J. Tan, A. Kumar, M. Gupta, and R. Singh, *Appl. Phys. Lett.* **123**(3), 033705 (2023).
- 6 S. M. R. Islam, D. Kwak, M. H. Kabir, M. Hossain, and K. S. Kwak, *IEEE Access* **3**, 678 (2015).
- 7 T. Chretiennot, D. Dubuc, and K. Grenier, *IEEE Trans. Microwave Theory Tech.* **61**, 972 (2013).
- 8 H. Lobato-Morales, A. Corona-Chavez, J. L. Olvera-Cervantes, R. A. Chavez-Perez, and J. L. Medina-Monroy, *IEEE Trans. Microwave Theory Tech.* **62**, 2160 (2014).
- 9 D. S. Filonov, E. I. Kretov, S. A. Kurdjumov, V. A. Ivanov, and P. Ginzburg, *J. Quant. Spectrosc. Radiat. Transfer* **235**, 127 (2019).
- 10 J. Scheuer, D. Filonov, T. Vosheva, and P. Ginzburg, *Opt. Express* **30**, 5192 (2022).
- 11 D. Filonov, S. Kolen, A. Schmidt, Y. Shacham-Diamand, A. Boag, and P. Ginzburg, *Phys. Status Solidi RRL* **13**, 1800668 (2019).
- 12 P. G. Darko Kajfez, *Dielectric Resonators* (Artech House Publishers, 1986).
- 13 A. Iqbal, A. Smida, O. A. Saraereh, Q. H. Alsafasfeh, N. K. Mallat, and B. M. Lee, *Sensors* **19**, 1200 (2019).
- 14 H. Cheng, X. Ren, S. Ebadi, Y. Chen, L. An, and X. Gong, *IEEE Sens. J.* **15**, 1453 (2015).
- 15 A. A. Mohd Bahar, Z. Zakaria, S. R. Ab Rashid, A. A. M. Isa, and R. A. Alahnomi, *Microwave Opt. Technol. Lett.* **59**, 367–371 (2017).
- 16 C. Liu and F. Tong, *IEEE Microwave Wireless Compon. Lett.* **25**, 751 (2015).
- 17 S. Mohammadi, K. K. Adhikari, M. C. Jain, and M. H. Zarifi, *IEEE Trans. Microwave Theory Tech.* **70**, 576 (2022).
- 18 A. Giorgini, S. Avino, P. Malara, P. De Natale, and G. Gagliardi, *Sensors* **19**, 473 (2019).
- 19 J. von Neumann and E. P. Wigner, *Phys. Z.* **30**, 467–470 (1929).
- 20 D. C. Marinica, A. G. Borisov, and S. V. Shabanov, *Phys. Rev. Lett.* **100**, 183902 (2008).
- 21 E. N. Bulgakov and A. F. Sadreev, *Phys. Rev. B.* **78**, 075105 (2008).
- 22 C. W. Hsu, B. Zhen, A. D. Stone, J. D. Joannopoulos, and M. Soljacic, *Nat. Rev. Mater.* **1**, 16048 (2016).
- 23 K. L. Koshelev, Z. F. Sadrieva, A. A. Shcherbakov, Y. S. Kivshar, and A. A. Bogdanov, *Phys. Usp.* **66**, 494 (2023).
- 24 M. Rybin and Y. Kivshar, *Nature* **541**, 164 (2017).
- 25 M. Odit, K. Koshelev, S. Gladyshev, K. Ladutenko, Y. Kivshar, and A. Bogdanov, *Adv. Mater.* **33**, 2003804 (2021).
- 26 A. Kodigala, T. Lepetit, Q. Gu, B. Bahari, Y. Fainman, and B. Kanté, *Nature* **541**, 196 (2017).
- 27 A. Nordin, *Nanobiosens. Dis. Diagn.* **5**, 41 (2016).
- 28 D. N. Maksimov, V. S. Gerasimov, S. Romano, and S. P. Polyutov, *Opt. Express* **28**, 38907 (2020).
- 29 I. Yusupov, D. Filonov, A. Bogdanov, P. Ginzburg, M. V. Rybin, and A. Slobozhanyuk, *Appl. Phys. Lett.* **119**, 193504 (2021).
- 30 Aldo Petosa, *Dielectric Resonator Antenna Handbook* (Artech, 2007).
- 31 D. Dobrykh, I. Yusupov, S. Krasikov, A. Mikhailovskaya, D. Shakirova, A. Bogdanov, A. Slobozhanyuk, D. Filonov, and P. Ginzburg, *IEEE Trans. Antennas Propag.* **69**(6), 3125–3131 (2021).
- 32 M. V. Rybin, K. L. Koshelev, Z. F. Sadrieva, K. B. Samusev, A. A. Bogdanov, M. F. Limonov, and Y. S. Kivshar, *Phys. Rev. Lett.* **119**, 243901 (2017).
- 33 E. A. Nenasheva, O. N. Trubitsyna, N. F. Kartenko, and O. A. Usov, *Phys. Solid State* **41**, 799 (1999).